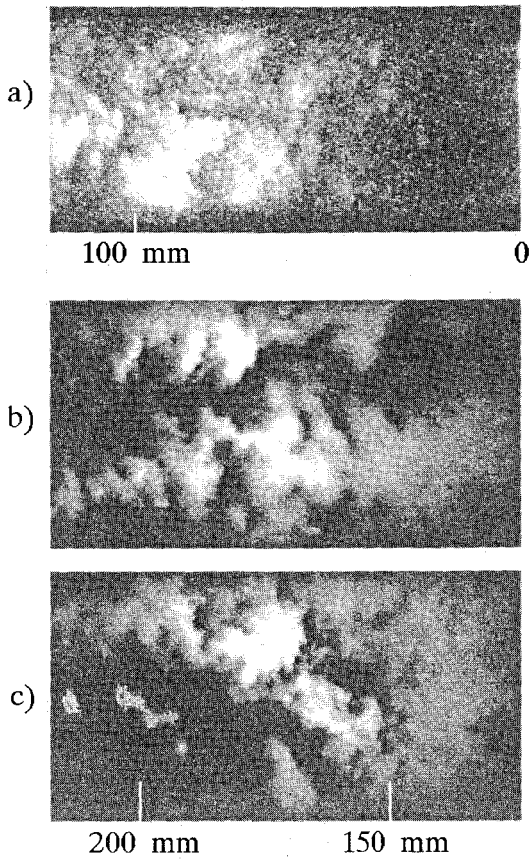

Fig. 5 Plan (*X-Z*) view in the developing (a) and fully developed (b and c) regions for $M_c = 0.86$.

Conclusions

Filtered Rayleigh scattering-based flow visualizations were used in compressible mixing layers. The lower compressibility case ($M_c = 0.51$) displays well-defined roller-type spanwise structures and streamwise streaks (perhaps indicative of streamwise vortices). The structures of the high compressibility case ($M_c = 0.86$) are more three dimensional and oblique. Work is currently underway to obtain quantitative information using this planar technique.

Acknowledgment

The support of NASA Lewis Research Center (NAG 3-764), the National Science Foundation (CTS-9006879), and the Office of Naval Research (N00014-90-J-1730) is greatly appreciated.

References

[1]Papamoshcou, D., and Roshko, A., "The Compressible Turbulent Mixing Layer: An Experimental Study," *Journal of Fluid Mechanics,* Vol. 197, 1988, pp. 453-477.

[2]Elliott, G. S., and Samimy, M., "Compressibility Effects in Free Shear Layers," *Physics of Fluids A,* Vol. 2, No. 7, 1990, pp. 1231-1240.

[3]Samimy, M., Reeder, M. F., and Elliott, G. S., "Compressibility Effects on Large Structures in Free Shear Flows," *Physics of Fluids A,* Vol. 4, No. 6, pp. 1251-1258.

[4]Elliott, G. S., Samimy, M., and Arnette, S. A., "A Study of Compressible Mixing Layers Using Filtered Rayleigh Scattering," AIAA Paper 92-0175, Jan. 1992.

[5]Clemens, N. T., and Mungal, M. G., "Two- and Three-Dimensional Effects in the Supersonic Mixing Layer," AIAA Paper 90-1978, July 1990.

[6]Sandham, N.D., and Reynolds, W.C., "Three-dimensional Simulations of Large Eddies in the Compressible Mixing Layer," *Journal of Fluid Mechanics,* Vol. 224, 1991, pp. 133-158.

[7]Miles, R. B., Lempert, W. R., and Forkey, J., "Instantaneous Velocity Fields and Background Suppression by Filtered Rayleigh Scattering," AIAA Paper 91-0357, Jan. 1991.

[8]Bernal, L. P., and Roshko, A., "Streamwise Vortex Structure in Plane Mixing Layers," *Journal of Fluid Mechanics,* Vol. 170, 1986, pp. 499-525.

Double Piston Shock-Wave Valve

H. Onodera*
Iwate University, Morioka 020, Japan

Introduction

THE shock tube is a useful tool for simulating shock-wave phenomena. In its early applications, it was used as a supersonic wind tunnel by utilizing the high-speed flow induced behind the incident shock wave. Recently, it has been used to generate plane shock waves since there has been a growing interest in the evolution and propagation of such shock waves.

There are many different methods for generating shock waves that produce high-speed gas flow, including using diaphragms, shock-wave valves, the free-piston gun tunnel, ballistic range (light gas gun), the Ludwieg tube, and electromagnetic systems. Of these various approaches the use of the diaphragm is the simplest and easiest to handle. However the production and changing of diaphragms is tedious and time consuming and causes various difficulties. Furthermore, during experiments part of the diaphragm might fly off into the shock-tube channel and test section, thereby disturbing the event to be observed (e.g., the shock-wave front and the air flow behind it). When this happens, the shock tube must be disassembled, the debris left from the diaphragm removed, and the apparatus reassembled. If metal diaphragms are used, damage to the shock-tube wall, observation windows, and/or test models may occur in extreme cases. When a poisonous gas is used as the test gas, or when there is a chemical shock tube, the rupture of the diaphragm can be extremely troublesome since the gas inside the shock tube may diffuse into the laboratory space when the ruptured diaphragm is being replaced for the following run. Replacing the lost gaseous atmosphere inside the tube can also be time consuming.

Diaphragm rupture is not always spontaneous; in many cases a needle is used to burst the diaphragm. In such cases, the shock-wave speed cannot be adjusted precisely since the velocity of the needle cannot be kept constant. However, precise wave-speed adjustment is essential for weak shock-wave research. This requirement is difficult to achieve when using a normal diaphrapm system.

A shock-wave valve is a suitable solution to the problem. Recently, some research regarding the development of shock-wave valves has been reported.[1-3] In the early types of shock-wave valves, the flow was forced to make a 180-deg turn at the valve. Subsequently, a system was proposed using a piston and valve arrangement such that the flow area at the valve remained constant[1,2]; thus the pressure losses were significantly reduced. However, this system was too complicated for easy and reliable use.

The purpose of the present Note is to introduce a new concept for a shock-wave valve. This valve has a simple structure, is easy to operate, and is suitable for large-scale shock tubes. It also generates very little turbulence in the flowfield produced.

Valve Design and Structure

The proposed shock-wave valve system is placed at the diaphragm position as shown in Fig. 1. This system is an independent unit, constituting a partition between the high-pressure chamber on one side and the low-pressure channel on the other side. It is different from the previous shock wave valve in that it can use whatever shock creating systems were

Received Dec. 11, 1991; revision received March 10, 1992; accepted for publication March 10, 1992.

*Research Associate, Department of Mechanical Engineering.

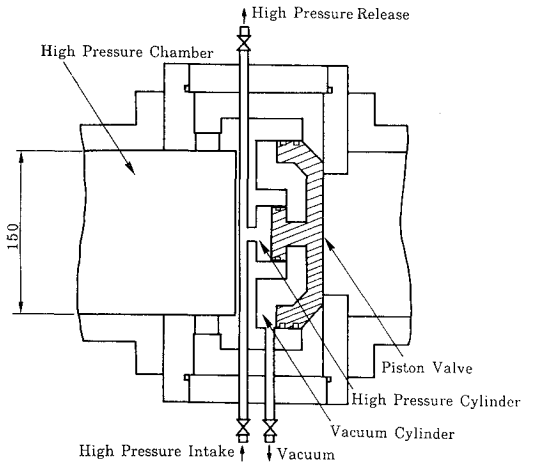

Fig. 1 Present shock-wave valve.

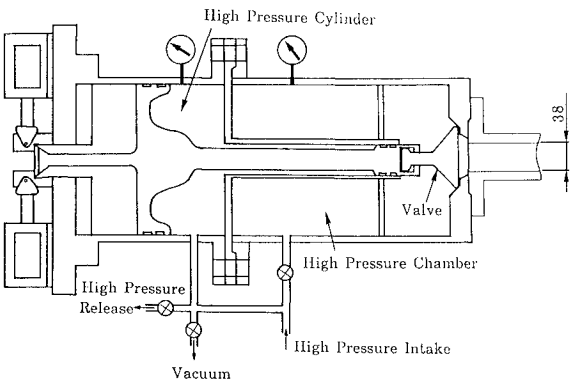

Fig. 2 Example of an earlier shock-wave valve.

used previously, and by changing the length of the high-pressure chamber one can obtain the required test time in the postshock flow.

A description of the operation of the proposed valve is now given. First the piston valve is moved to the extreme left by evacuating the vacuum cylinder (118.9 cm^3). At this time, the high-pressure release valve is opened. Next we apply pressure to the high-pressure cylinder, whose volume (7.36 cm^3) is only 6.2% of the volume of the vacuum cylinder, with the high pressure overcoming the negative pressure of the vacuum cylinder. The next step is to apply the driver gas until the required pressure is reached in the high-pressure chamber. The piston valve can now be activated by quickly dumping the gas inside the high-pressure cylinder by means of the high-pressure release valve. This causes the piston valve to start moving rapidly toward the left because of the pressure difference between the atmospheric pressure in the shock tube and the subatmospheric pressure in the vacuum cylinder. As a result of this movement, the driver gas discharges immediately into the low-pressure channel and forms the shock-wave front.

An example of previous shock-wave valve designs[1-3] is the design of Ref. 1, which is typical of the concept used. As shown in Fig. 2, it can be seen that the number of parts, especially moving parts, of the system is large. For this reason, this type of design is not suitable for large-scale shock tubes.

In the system considered in this Note, the piston valve is released by high-pressure dumping, but the volume of the cylinder is quite small, so that the pressure dump is effected easily and rapidly. Moreover, the pressure difference between the vacuum cylinder and the channel is large, and the area that is subjected to the piston driving pressure is sufficiently large. Therefore, even with the heavy piston valve that is required for a large-scale shock tube, the valve releases rapidly. [For reference, the mass of the piston valve (1 kg) is about four times greater than in previously used[1] piston valves.]

Note that in the present system the operating time of the valve will become longer if the channel pressure is negative, since the pressure difference between the two sides of the piston valve decreases.

Performance Data of the Present Shock-Wave Valve

The formation of the shock wave produced by the proposed valve was measured using pressure transducers (Kistler 603B) arranged as shown in Fig. 3. The data gathered during an experiment were stored in a digital wave memory (Asunogiken AS-1000, 16 kword, 9 ch) with a sampling rate of 2 μs/word (point). The data were analyzed with a personal computer (NEC PC9801VX). The cross section of the shock tube low-pressure channel used was 60 × 150 mm and 8.3 m long.

Figure 4 shows the case of the pressure ratio between the high-pressure chamber and the low-pressure channel $P_{41} = 2.5$, and the pressure of the high-pressure cylinder $P_h = 18.5$ kgf/cm^2 (1.8 MPa). Helium was used in the high-pressure cylinder, since its molecular weight and flow resistance are low. The driven gas was atmospheric pressure air. Numbers in the figure correspond to the transducer numbers that are shown in Fig. 3. Even at location 1 (6137 mm from the valve) a well-formed discontinuity occurs. At location 9 the available test time for the flow behind the incident shock wave is more than 900 μs. In this performance, shock Mach number M_s is about 1.2. This value is comparable to the normal diaphragm-type shock tube. Moreover, the pressure signature behind the shock-wave front is reasonably smooth.

Figure 5 shows the dependence of the incident shock-wave Mach number on the nondimensionalized distance L/D, where D is the calculated diameter of the shock tube. (The shock tube is 107 mm in diameter calculated in terms of the pipe.) The pressure ratio P_{41} appears as a parameter. The gases in brackets denote the driver gases used.

The nondimensionalized shock formation lengths are L/D = 70 for M_s = 1.12, and 65 for M_s = 1.19 and 1.2, respectively. For M_s = 1.12 and 1.19, a grid was inserted 5717 mm away

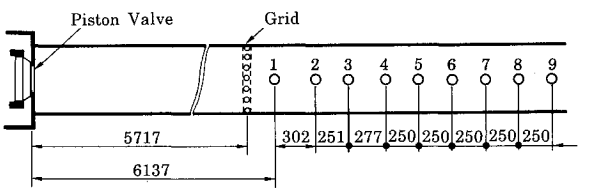

Fig. 3 Pressure transducer arrangement.

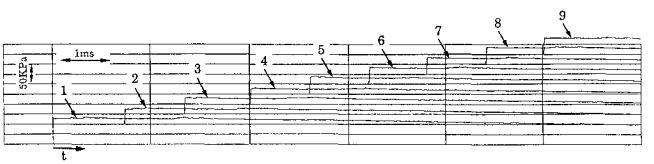

Fig. 4 Formation of shock wave, P_{41} = 2.5, P_h = 18.5 kgf/cm^2.

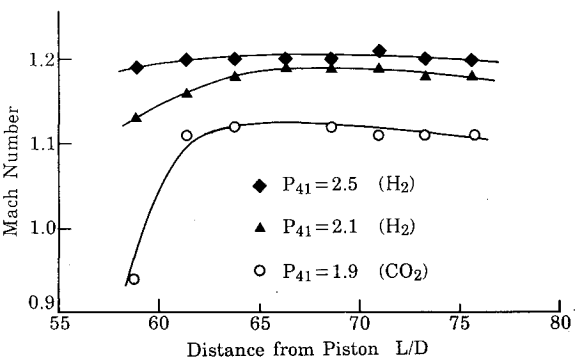

Fig. 5 Shock-wave Mach number vs nondimensionalized distance.

from the piston valve to accelerate the formation of the shock-wave front. In previously suggested valve designs, values of L/D from 20 to 40 for $M_s = 1.61$ were quoted.[2] It is apparent that the present valve system exhibits good performance even with a heavy piston valve while having a relatively simple structure.

Obtained shock-wave Mach numbers are almost the same values as the analytical ones. In previous shock-wave valve designs,[2] the obtained shock-wave Mach number was between 60 and 90% of the analytical value.

Conclusions

To overcome the defects of diaphragm-type shock tubes, a double-piston-type shock-wave valve has been designed and constructed. The results obtained from the proposed new valve are summarized as follows.

1) Even though this valve has a simple design and the piston is comparatively heavy, smooth postshock pressures were obtained for incident shock-wave Mach numbers of $M_s = 1.2$ and higher.

2) Shock-wave formation length is about 65 calculated shock-tube diameters for $M_s = 1.2$; this is comparable to what is obtained with other types of shock-wave valves.

3) The Mach number obtained with this valve is very close to analytically predicted values, and the pressure loss at the valve is small.

Acknowledgments

The author would like to express his gratitude to K. Takayama of the Institute of Fluid Science, Tohoku University, for his encouragement throughout the course of the present report. The author is also indebted to O. Onodera for his assistance in conducting the present experiments.

References

[1]Ikui, H., Matsuo, K., and Yamamoto, Y., "A Study of Rapid Open Valve for Shock Tube I," *Transactions of the Japan Society of Mechanical Engineers,* Vol. 42, No. 359, July 1976, pp. 2127–2132.

[2]Ikui, H. et al., "A Study of Rapid Open Valve for Shock Tube II," *Transactions of the Japan Society of Mechanical Engineers,* Vol. 44, No. 385, Sept. 1978, pp. 3109–3115.

[3]Goebbels, D., Gavern, W., Synofzik, R., Wortberg, G., and Frohn, A., "The Generation of Very Weak Shock Waves and of N-Waves in a Shock tube," *Proceedings of the 11th International Symposium on Shock Tube and Waves,* Shock Wave Research Comittee, Seattle, WA, 1977, pp. 610–614.

Role of Matrix in Viscoplastic Behavior of Thermoplastic Composites at Elevated Temperature

Seung Jo Kim* and Jin Yeon Cho†
Seoul National University, Seoul 151-742, Korea

Introduction

THE ductility of thermoplastic resin improved the mechanical and environmental characteristics of fiber composites but induced the complicated viscoplastic behavior of fiber composites. Viscoplastic behavior is intrinsically nonlinear and the anisotropy of composites increases the difficulties of describing the viscoplastic behavior of thermoplastic composites. Therefore, to use the thermoplastic composites properly, the viscoplastic behavior of thermoplastic composites must be studied more thoroughly. And also the role of a matrix in viscoplastic behavior of thermoplastic composites needs to be investigated since the viscoplasticity of thermoplastic composites is from the ductility of thermoplastic resin.

Many studies[1-3] were reported for describing the nonlinear behavior of fiber composites. But the role of a matrix in viscoplastic behavior of thermoplastic composites was not investigated sufficiently in previous studies. In this study, to investigate the role of a matrix in viscoplastic behavior of thermoplastic composites, the concept, what we call "unmixing-mixing," is suggested. This concept makes us use not viscoplastic rule of anisotopic material (composite) but viscoplastic rule of isotropic material (matrix). Since many physical observations show that fibers deform linear elastically and matrices exhibit viscoplastic behavior, it can be said that the viscoplastic behavior of a matrix is the main factor in viscoplastic behavior of overall thermoplastic composites. Moreover, fiber composite is a mixture of isotropic materials (fiber and matrix). Thus, it is meaningful and plausible that the viscoplastic behavior of thermoplastic composites be predicted by using a viscoplastic rule of isotropic material (matrix).

Concept of "Unmixing and Mixing"

The following assumptions are used in this study.

1) Unidirectional composites considered in this study are in the plane stress state.

2) Strains of matrix and fiber are the same in fiber direction.

3) Total strain rate can be decomposed into elastic and plastic components.

4) Fibers and matrices exhibit linear elastic and viscoplastic behaviors, respectively.

To describe the elastic properties of composites in terms of constituent properties and to satisfy the above assumptions, the rule of mixture[4] in micromechanics is used. This rule of mixture considers the effect that the Poisson's ratio difference of fiber and matrix induces force in fiber direction under transverse loading conditions. The rule of mixture is as follows:

$$E_1 = E_f V_f + E_m V_m \tag{1a}$$

$$\nu_{12} = \nu_f V_f + \nu_m V_m \tag{1b}$$

$$1/E_2 = V_f/E_f + V_m/E_m - V_f V_m(\nu_f^2 E_m/E_f + \nu_m^2 E_f/E_m - 2\nu_f\nu_m)/(E_f V_f + E_m V_m) \tag{1c}$$

$$1/G_{12} = V_f/G_f + V_m/G_m \tag{1d}$$

where V denotes the volume fraction. Subscript f and m denote fiber and matrix, respectively, and subscript 1 and 2 denote the material principal axes (fiber direction and transverse direction). The effect of Poisson's ratio difference is presented in the third right-hand side term for E_2.

From the assumptions 2, 3, and 4 with kinematic observations, strain rates in (1,2) coordinate can be expressed in terms of elastic and plastic components.

$$\dot{\epsilon}_{11} = \dot{\epsilon}^e_{f_{11}} = \dot{\epsilon}^e_{m_{11}} + \dot{\epsilon}^p_{m_{11}} \tag{2a}$$

$$\dot{\epsilon}_{22} = V_f\dot{\epsilon}^e_{f_{22}} + V_m(\dot{\epsilon}^e_{m_{22}} + \dot{\epsilon}^p_{m_{22}}) = \dot{\epsilon}^e_{22} + V_m\dot{\epsilon}^p_{m_{22}} \tag{2b}$$

$$\dot{\epsilon}_{12} = V_f\dot{\epsilon}^e_{f_{12}} + V_m(\dot{\epsilon}^e_{m_{12}} + \dot{\epsilon}^p_{m_{12}}) = \dot{\epsilon}^e_{12} + V_m\dot{\epsilon}^p_{m_{12}} \tag{2c}$$

where superscript e and p denote elastic component and plastic component, respectively. The 1-direction strains of matrix and fiber are obtained from the elastic stress-strain relations with the assumptions 1, 3, and 4.

$$\dot{\epsilon}_{f_{11}} = \dot{\epsilon}^e_{f_{11}} = \dot{\sigma}_{f_{11}}/E_f - (\nu_f/E_f)\,\dot{\sigma}_{f_{22}} \tag{3a}$$

$$\dot{\epsilon}_{m_{11}} = \dot{\epsilon}^e_{m_{11}} + \dot{\epsilon}^p_{m_{11}} = \dot{\sigma}_{m_{11}}/E_m - (\nu_m/E_m)\,\dot{\sigma}_{m_{22}} + \dot{\epsilon}^p_{m_{11}} \tag{3b}$$

Received Sept. 6, 1991; revision received March 12, 1992; accepted for publication March 12, 1992.

*Associate Professor, Department of Aerospace Engineering.
†Research Assistant, Department of Aerospace Engineering.